

Gašparović, B., Penezić, A., Lampitt, R.S., Sudasinghe, N., Schaub, T. 2018. Phospholipids as a component of the oceanic phosphorus cycle. *Mar. Chem.* 250, 70-80.

Pre-print version

1 Phospholipids as a component of the oceanic phosphorus cycle

2 Blaženka Gašparović^{a,*}, Abra Penezić^a, Richard S. Lampitt^b, Nilusha Sudasinghe^{c,d}, Tanner Schaub^c

3 ^a *Division for Marine and Environmental Research, Ruđer Bošković Institute, POB 180, HR-10002*
4 *Zagreb, Croatia*

5 ^b *National Oceanography Centre, Southampton, United Kingdom SO14 3ZH*

6 ^c *College of Agricultural, Consumer and Environmental Sciences, New Mexico State University, United*
7 *States*

8 ^d *Bioscience Division, Los Alamos National Laboratory, Los Alamos, NM 87545, United States*

9 *Correponding author. Tel.: +385 1 4561 148; fax: +385 1 4680 242

10 E-mail address: gaspar@irb.hr (Blaženka Gašparović).

11

12 **Abstract**

13 We characterize the distribution of oceanic phosphorus-containing lipids (PL) in the Northeast Atlantic
14 by Iatroscan thin layer chromatography and high resolution Fourier transform ion cyclotron resonance
15 mass spectrometry (FT-ICR MS). Phospholipids are a small but significant fraction of oceanic particulate
16 organic carbon (POC) (1.5%). We describe the distribution of 1,862 PL compounds in total, of which only
17 ~27% have elemental compositions that match those found in the Nature Lipidomics Gateway database
18 (e.g., phosphatidylglycerol (PG), phosphatidylcholine (PC), phosphatidylethanolamine (PE), phosphatidic
19 acid (PA), phosphatidyl serine (PS), and phosphatidylinositol (PI)). The highest phospholipid
20 concentration is found in the epipelagic, which reflects primary production in that depth horizon. Depth-
21 related PL removal was the strongest for PL signals that match database-reported (known) lipids and was
22 lower for saturated non-database (novel) matched PL. The transformation of known PL is marked by
23 depth-related increase in saturation with PA that is assumed to be generated as the earliest transformation
24 product of PL. Novel unsaturated P-lipids likely originate from both PL transformation processes and *in-*
25 *situ* biological production at the surface layer. Novel PL are dominated by unsaturated compounds for
26 which unsaturation increased between the epipelagic (average molecular double bond equivalents,
27 DBE=5) and the abyssopelagic (average DBE=6.7) zones. Additionally, those compounds increase in both
28 average molecular weight and contribution to all lipid content with increasing depth, likely from cross-
29 linking of unsaturated compounds. Our data indicate that novel PL are selectively preserved with depth
30 and therefore are P and C carriers to the deep Atlantic. We demonstrate that a full appreciation of

Gašparović, B., Penezić, A., Lampitt, R.S., Sudasinghe, N., Schaub, T. 2018. Phospholipids as a component of the oceanic phosphorus cycle. *Mar. Chem.* 250, 70-80.

Pre-print version

31 phosphorus cycling requires additional data on phospholipid composition and especially the ecological
32 role and depth-related molecular change of these compounds.

33 *Keywords:* Phospholipids; phospholipid depth-related transformations; FT-ICR MS, TLC/FID;
34 Northeast Atlantic Ocean

35 **Introduction**

36 Phosphorous (P) is an essential nutrient for phytoplankton growth and in places limits oceanic
37 primary production (Moore et al., 2013, Wu et al., 2000; Yoshimura et al., 2007). Phosphorus is a
38 component of key molecules such as nucleic acids, phospholipids, ATP and complex carbohydrates.
39 Unlike nitrogen, which can be supplied by nitrogen fixation in the euphotic zone, the supply of other
40 macro-nutrients is dominated by deep mixing and upwelling (Dugdale and Goering, 1967). Phosphorus
41 supply to the ocean depends on continental input. River runoff represents the main phosphorus source in
42 the ocean (Baturin, 2003). However, there is no atmospheric reservoir of phosphorus. Moreover, the
43 phosphorus budget of the ocean is unbalanced since the accumulation of phosphorus in marine sediments
44 and altered oceanic crust exceeds the continental input of particulate and dissolved phosphorus
45 (Wallmann, 2010).

46 Various chemical forms of P participate in numerous abiotic and biotic processes collectively
47 referred to as the P cycle, which is strongly connected to the carbon cycle and therefore to the capability
48 of oceans for climate change mitigation due to their capacity to sequester carbon from the atmosphere. A
49 crucial process in this is the generation of carbon-rich material in the upper ocean. The particles export a
50 fraction of the primary production out of the euphotic zone (i.e. the “biological carbon pump”). Export
51 flux of POC is less than 5-10% of total primary production in the ocean (Buesseler, 1998). Any organic
52 carbon that escapes mineralization in this environment is liable to be sequestered for millennia, ultimately
53 representing the sequestration of atmospheric CO₂ (Lampitt et al., 2008). Microorganisms are primarily
54 responsible for carbon (Azam, 1998) and P (Karl, 2014) assimilation and remineralization in the ocean.

55 Lipids are a major biochemical class in seawater along with carbohydrates and proteins. They are
56 carbon rich, with a high energetic value, and thus represent important metabolic fuels. Phosphorus
57 containing lipids (i.e. phospholipids) are a major component of cell membranes that provide structure and
58 protection to cells. Membrane lipids generally contribute to 15 to 25% of the carbon in planktonic cells

Gašparović, B., Penezić, A., Lampitt, R.S., Sudasinghe, N., Schaub, T. 2018. Phospholipids as a component of the oceanic phosphorus cycle. *Mar. Chem.* 250, 70-80.

Pre-print version

59 (Wakeham et al., 1997). The synthesis of phospholipids consumes 18-28% of the PO_4^{3-} taken up by the
60 total planktonic community in the North Pacific subtropical gyre (Van Mooy et al., 2006). The proportion
61 of PL in phytoplankton varies widely from a few percent to as much as half of the total lipid content.
62 Nutrient conditions affect the composition of cellular lipid composition in phytoplankton; diatoms grown
63 under nutrient replete conditions exhibit high proportions of PL, while in P-depleted conditions PL content
64 is dramatically reduced (Geider and La Roche, 2002; Martin et al., 2011a). Phospholipids comprise a
65 significant proportion of cellular phosphorus (e.g., 36% and 15-20% of cellular P of the freshwater
66 phytoplankton *Ankistrodesmus falcatus* (Geider and La Roche, 2002) and marine bacteria (Dobbs and
67 Findlay, 1993) respectively. On average, PL account for $4\pm 1\%$ and $7.1\pm 2.5\%$ of the total particulate
68 phosphorus in the eastern subtropical South Pacific and in the Mediterranean, respectively (Van Mooy
69 and Fredrichs, 2010, Poppendorf et al., 2011). Dominant phospholipid molecules vary by plankton
70 species. Heterotrophic bacteria are the dominant sources of phosphatidylglycerol (PG) and
71 phosphatidylethanolamine (PE), while PC phosphatidylcholines (PC) are derived primarily from
72 eukaryotic phytoplankton (Van Mooy and Fredrichs, 2010).

73 Phospholipid concentration varies between marine environments. Particulate PL concentrations in
74 the northern Adriatic, Mediterranean, throughout a year vary in the range of 3.0 to 27.7 $\mu\text{g/l}$, with a
75 contribution to total lipids between 17.8 and 50.3% (Frka et al., 2011; Marić et al., 2013) as measured by
76 thin layer chromatography. PL in the oligotrophic to mesotrophic region of the east Atlantic, measured by
77 thin layer chromatography, ranged from 1.3 to 7.8 $\mu\text{g/l}$, contributing between 11.4 and 55.0% of total lipid
78 content (Gašparović et al., 2014). In the upper 250 m of the oceanic water column, concentrations of
79 measured PL (PG+PE+PC) in the eastern subtropical South Pacific ranged between 130-1350 pmol/l (Van
80 Mooy and Fredrichs, 2010). The depth distribution of the three phospholipids (PG, PE, and PC) across the
81 Mediterranean Sea was quite similar, each phospholipid class was approximately 200–600 pmol/l in the
82 surface, increasing to 200–800 pmol/l at 50–75 m, then decreasing to 100–200 pmol/l at 250 m (Poppendorf
83 et al., 2011). There is a wide variability in P-related physiology among marine plankton, including the
84 ability to acquire and utilize different organic P sources (Ivančić et al., 2012), and the substitution of PL
85 with non-phosphorus lipids in P-limited conditions (Van Mooy et al., 2009; Sebastián et al., 2016).

86 The transformation processes of phosphorus-containing molecules within the water column remain
87 poorly understood (Benitez-Nelson, 2000), particularly related to their degradation (Rontani et al., 2009;

Pre-print version

88 Rontani et al., 2012). To our knowledge, there are no published reports on oceanic phospholipid
89 degradation processes, but they are clearly an essential resource for some deep ocean organisms that are
90 unable to synthesise them (Mayor et al., 2013; Pond et al., 2014).

91 .

92 Given the importance of P as a major limiting nutrient, we are interested in the surface Atlantic
93 production of phospholipids and their potential as a phosphorus and carbon carrier to the deep ocean.
94 There is a pressing need to understand the processes involved in the early transformation of PL that are
95 responsible for chemical change in terms of both concentration and molecular characteristics. To address
96 this issue we performed complete phospho-lipidomic analysis by direct-infusion FT-ICR MS. Molecular
97 formulae are derived directly from FT-ICR MS measurement and subsequently matched to a lipid
98 database. While this approach neglects isomeric identification, it is the only measure available that
99 provides global description for multiple thousands of organic molecules in these environments. With these
100 data, we characterize the nature of particulate PL, their removal and transformations through the water
101 column. In addition we used thin-layer chromatography with flame ionization detection to quantitatively
102 detect total lipid and bulk phospholipid to complement the FT-ICR MS analysis and illuminate the modern
103 P cycle.

104

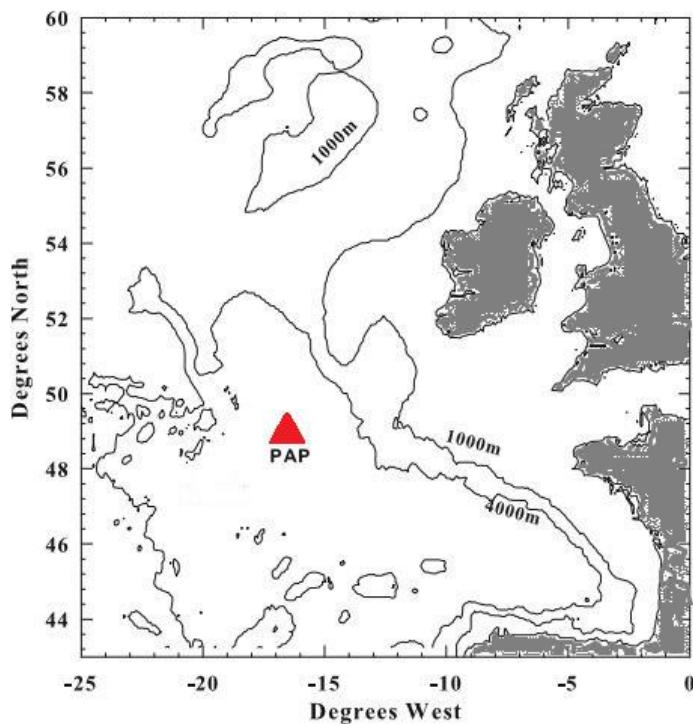
105 **Methods**

106 **2.1. Location**

107 The study site, of the Porcupine Abyssal Plain Sustained Observatory (PAP-SO) in the Northeast
108 Atlantic (49N, 16.5W) (Fig. 1) has been the main focus of many studies since 1992. This region is isolated
109 from the complexities of the continental slope and the Mid-Atlantic Ridge. A persistent feature of the
110 North Atlantic is undersaturation of CO₂ in surface waters throughout the year, which gives rise to a
111 perennial CO₂ sink and makes this a region of great importance in the global carbon cycle (Hartman et al.,
112 2012). In terms of biogeographical provinces that have dynamical boundaries, it is well within the North
113 Atlantic Drift (NADR) province (Longhurst, 2007), which is generally characterized with spring bloom
114 that is developing from the late April, starting at the southern part of NADR and progressing northward
115 until June. The influences of the continental shelves and slope are thought to be slight at PAP with

Pre-print version

116 negligible advection of particulate material (Weaver et al., 2000). Eddy activity is much lower than in
117 many other oceanic regions (Chelton et al., 2007), and such as they are, they tend not to traverse quickly.
118 Currents are generally weak (Lampitt et al., 2001) and lateral advection speeds are low but significant
119 (Williams et al., 2006; Hartman et al., 2010).



120
121 Fig. 1. PAP sampling site.

122
123 **2.2. Sample processing**

124 Sampling was conducted at the PAP station from the RRS James Cook on June 14, 2013. Ocean
125 samples were collected at 21 depths from the surface (2 m) to 4800 m (50 m above bottom) (epipelagic
126 (0-100 m), mesopelagic (100-1000 m), bathypelagic (1000-4000 m) and abyssopelagic (4000-4900 m))
127 from a pre-dawn (~0400 local time) Seabird 911+ CTD-Niskin rosette. Six of the surface sampled depths
128 (2-100 m depth) corresponded to 97, 55, 20, 7, 5 and 1% of surface irradiance intensity.

129 Particulate lipids were collected on board on 0.7 μm Whatman GF/F filters combusted at 450°C/5h
130 by filtering 5-10 l of oceanic water at 12 kPa vacuum pressures immediately after sampling and stored at
131 -80°C until analysis.

132

133 **2.3. Basic environmental parameters**

134 Temperature, salinity, and oxygen measurements were made using Seabird SBE 37-IM recorders
135 (Sea-Bird Electronics Inc., Bellevue, Washington, USA). Samples for nutrient (total inorganic nitrogen
136 (TIN= nitrate (NO_3^-) + nitrite (NO_2^-) + ammonium (NH_4^+)), orthophosphate (PO_4^{3-}) and orthosilicate
137 (SiO_4^{4-})) analysis were drawn into 25 ml plastic coulter counter vials from Niskin bottles. The vials were
138 stored in the dark at 4°C until analysis, which commenced within 24 hours of sampling. Nutrients were
139 determined in triplicate in unfiltered water samples with a Skalar Sanplus segmented flow autoanalyzer
140 and standard colorimetric techniques described by Kirkwood (1996).

141 Fluorometric measurements of total Chlorophyll *a* (Chl *a*) were made on board by filtration of 250
142 ml of seawater through Whatman GF/F (nominal pore size 0.7 μm) glass fibre filters, extraction of the
143 filters in 10 ml of 90% acetone (HPLC grade) for 18–20 h (dark, 41°C) and determination of chlorophyll
144 fluorescence with a TD-700 (Turner Designs) fluorimeter (after Welschmeyer, 1994). Size-fractionated
145 Chl *a* measurements were made by sequential filtering of 1.2 l of seawater through 10 and 2 μm
146 polycarbonate filters (Fieder Filter Systems, UK), and extraction with GF/F filters to provide a
147 comparison between micro- and nanophytoplankton derived Chl *a*. Filtering was performed on board and
148 filters were stored at -80°C until analysis.

149

150 **2.4. Lipid extraction and measurements**

151 Lipids were extracted on land by a modified one-phase solvent mixture of dichloromethane –
152 methanol - water procedure (1:2:0.8, v:v:v) (Blight and Dyer, 1959). One μg of the internal standard
153 reserpine was added to each sample before extraction for FT-ICR MS. Mass spectral peak magnitude for
154 each compound was normalized (in both modes) to the internal standard (i.e. reserpine) peak magnitude,
155 so that the mass spectral signals for each compound could be normalized to a fixed volume of seawater.
156 Ten μg of hexadecanone was added to each sample before extraction for Iatroscan analysis. This internal
157 standard was then extracted with the lipids in the sample, and the amount measured in the final concentrate
158 provided an estimate of lipid recovery. The lipid extraction efficiency was between 81 and 105%. Extracts
159 were concentrated by rotary evaporation and brought to dryness under a nitrogen atmosphere.

Pre-print version

160 The particulate-derived lipid material collected was analyzed by direct-infusion electrospray
161 ionization Fourier transform ion cyclotron resonance mass spectrometry (ESI FT-ICR MS) in both
162 negative and positive ionization mode to provide elemental composition determination for lipids that can
163 serve as diagnostic markers for their origin, transformation and preservation potential through the ocean
164 water column. ESI FT-ICR mass spectrometry was performed with a hybrid linear ion trap 7 T FT-ICR
165 mass spectrometer (LTQ FT, Thermo Fisher, San Jose, CA) equipped with an Advion Triversa Nanomate
166 (Advion Biosystems, Inc.) as previously described (Holguin and Schaub, 2013). FT-ICR mass spectra
167 were acquired at a mass resolving power of $m/\Delta m_{50\%} = 400,000$ at m/z 400 (i.e. a time-domain
168 acquisition period of ~ 3 s). A total of 500 time-domain transients were co-added for each sample in both
169 positive and negative ionization modes prior to fast Fourier transformation and frequency to mass-to-
170 charge ratio conversion. FT-ICR mass spectra were internally calibrated to achieve sub part-per-million
171 mass measurement accuracy which facilitates direct assignment of elemental composition from measured
172 m/z ratio and peak lists were generated from each mass spectrum at $S/N > 10$. Internal calibration of the
173 mass spectra was performed using homologous alkylation series of known compounds where elemental
174 compositions differ by integer multiples of CH_2 . High-resolution FT-ICR mass spectra confirm that all
175 observed ions are single charged as evidenced by the 1 Da spacing between $^{12}\text{C}_c$ and $^{13}\text{C}_1$ $^{12}\text{C}_{c-1}$ peaks for
176 the species with the same molecular formula. IUPAC measured masses ($\text{CH}_2 = 14.01565$ Da) were
177 converted to the Kendrick mass scale ($\text{CH}_2 = 14.0000$ Kendrick mass units) as previously described
178 (Kendrick, 1963) and sorted by the Kendrick mass defect to facilitate identification of homologous series
179 with the same heteroatom composition and the same double-bond equivalents (DBE) but differing in the
180 degree of alkylation. DBE was calculated as follows: $\text{DBE} = \text{C} + 1 - \text{H}/2 + \text{N}/2$ (halogens omitted because
181 they were not observed in our analysis). Mass spectral peak magnitude for each compound was normalized
182 (in both modes) to the internal standard (i.e. reserpine) peak magnitude, so that the mass spectral signals
183 for each compound could be normalized to a fixed volume of seawater.

184 High mass measurement accuracy and mass resolving power combined with Kendrick mass sorting
185 and isotopic fine structure analysis enables robust determination of elemental compositions for individual
186 lipid compounds present in these extracts. Derived elemental compositions are matched to an in-house
187 assembled lipid library derived from Lipid Maps (<http://www.lipidmaps.org/>). For the purposes of this
188 paper, elemental compositions for which multiple database isomeric matches are possible, further
189 identification was not attempted. In cases where we discuss specific lipid molecular classes, those

Pre-print version

190 compounds represent elemental compositions for which only one database match is made. Relative
191 abundance for certain PL class is calculated by normalization of that PL class peak magnitude at each
192 depth to the lowest measured that PL peak magnitude across the depth profile. Compounds for which
193 elemental composition matches one or more lipid in the database are termed “database-matched” or
194 “known” and non-database matched compounds are termed “novel” for this discussion.

195 Additionally, total lipid and lipid class quantitation was performed by IATROSCAN thin layer
196 chromatography/flame ionization detection (TLC/FID) (Iatroscan MK-VI, Iatron, Japan). Lipids were
197 separated on silica-coated quartz thin-layer chromatography (TLC) rods (Chromarods SIII) (SES–
198 Analyseysteme, Germany) and quantified by an external calibration with a standard lipid mixture. The
199 lipid class quantification was achieved using calibration curves obtained for a standard by plotting peak
200 area against lipid amount spotted. Hydrogen flow rate was 160 ml/min and air flow rate was 2000 ml/min.
201 Each lipid extract was analyzed in duplicate: for the analysis, 2 µl aliquots of 20 µl of the solution in
202 dichloromethane were spotted by semiautomatic sample spotter. The standard deviation determined from
203 duplicate runs accounted for 0–9% of the relative abundance of lipid classes.

204 The separation scheme of 18 lipid classes involve subsequent elution steps in the solvent systems of
205 increasing polarity. For the separation of PG, PE and PC last two solvent system including solvent mixture
206 acetone–chloroform–methanol–formic acid (33:33:33:0.6, v:v:v:v) during 40 min for PG separation.
207 Finally, solvent mixture chloroform-methanol-ammonium hydroxide (50:50:5, v:v:v) during 30 min
208 allowed separation of PE and PC, and non-lipid material which remained at the origin. Total lipid
209 concentration was obtained by summing all lipid classes quantified by TLC-FID. Details of the procedure
210 are described in Gašparović et al. (2015; 2017).

211

212 2.5. Particulate organic carbon analysis

213 Seawater samples (1 l) collected from the CTD rosette were prepared by filtering onto combusted
214 25 mm GF/F filters and stored on board at –20 °C for subsequent particulate organic carbon (POC)
215 analysis. Inorganic carbonates were removed from the filters by acidification with fuming concentrated
216 hydrochloric acid. The filters were dried in the oven at 50 °C for 24 h, packaged in pre-combusted tin
217 capsules and analysed with an Automated Nitrogen Carbon Analysis for Gas, Solids and Liquids (ANCA-
218 GSL) preparation system coupled to a PDZ Europa 20-20 Stable Isotope Analyzer (PDZ Europa Scientific

Gašparović, B., Penezić, A., Lampitt, R.S., Sudasinghe, N., Schaub, T. 2018. Phospholipids as a component of the oceanic phosphorus cycle. *Mar. Chem.* 250, 70-80.

Pre-print version

219 Instruments, Northwich, UK). The mass spectrometer can be tuned using source settings for sensitivity
220 and/or linearity of a standard range. A typical standard range used for linearity is 25–1028 μg carbon, the
221 limit of detection being 3 times the standard deviation of the blank of an analysis. The blank consisting of
222 a tin capsule is analyzed in triplicate.

223

224 2.6. Pigment analysis

225 Pigment data are derived from the same set of FT-ICR MS data as for phospholipids (*c.f.* paragraph
226 2.4).

227

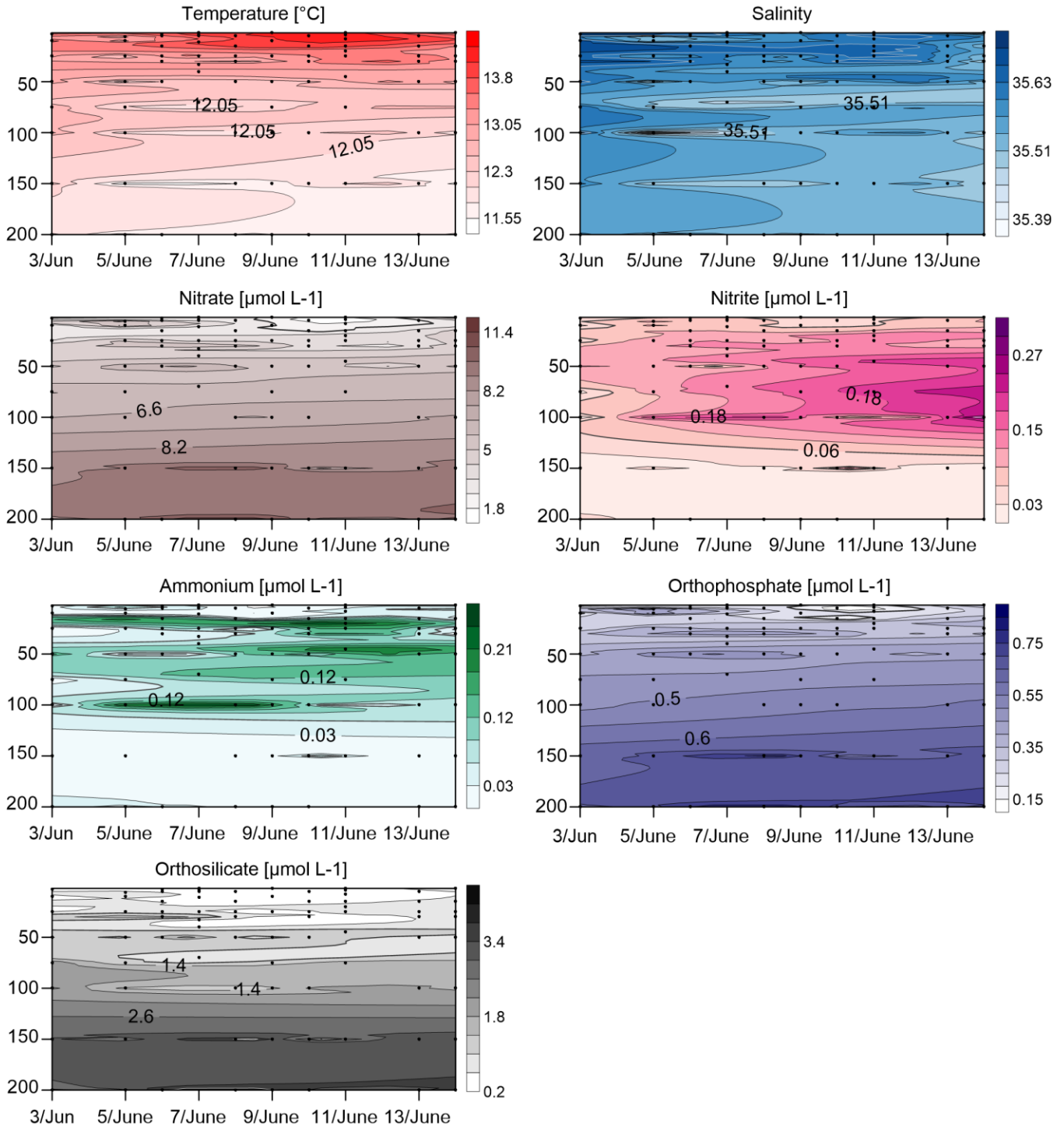
228

229 **Results**

230 Environmental conditions during the cruise to the PAP-SO from May 31st to June 18th, 2013 are
231 presented in Fig. 2. Although sampling was performed on the penultimate day of the cruise period, we
232 present environmental conditions for the whole cruise period to get insight into conditions that preceded
233 PL production and their export to the deep ocean. We assume that PL found below the euphotic zone were
234 produced during the previous days. During the course of the cruise the temperature decreased from 14.3
235 to 11.3°C from the surface to 200 m, while salinity varied slightly between 35.35 and 35.70.
236 Orthophosphate concentration increased with depth from 0.01 to 0.88 $\mu\text{mol L}^{-1}$ (average 0.44 $\mu\text{mol L}^{-1}$)
237 and the TIN concentrations were in the range of 0.26 to 12.26 $\mu\text{mol L}^{-1}$ (average 5.09 $\mu\text{mol L}^{-1}$). SiO_4^{4-}
238 concentration increased from 0.06 to 6.58 $\mu\text{mol L}^{-1}$ from the surface to 250 m depth (average 1.15 $\mu\text{mol L}^{-1}$)
239 and the surface productive layer (0-50 m) showed a low concentration of SiO_4^{4-} with an average
240 concentration of 0.65 $\mu\text{mol L}^{-1}$. There is a continuous concentration increase of all nutrients from 250 m
241 to 4800 m depth, reaching concentrations of 22.99 $\mu\text{mol L}^{-1}$ TIN, 1.89 $\mu\text{mol L}^{-1}$ PO_4^{3-} and 44.35 $\mu\text{mol L}^{-1}$
242 SiO_4^{4-} (Gašparović et al., 2017).

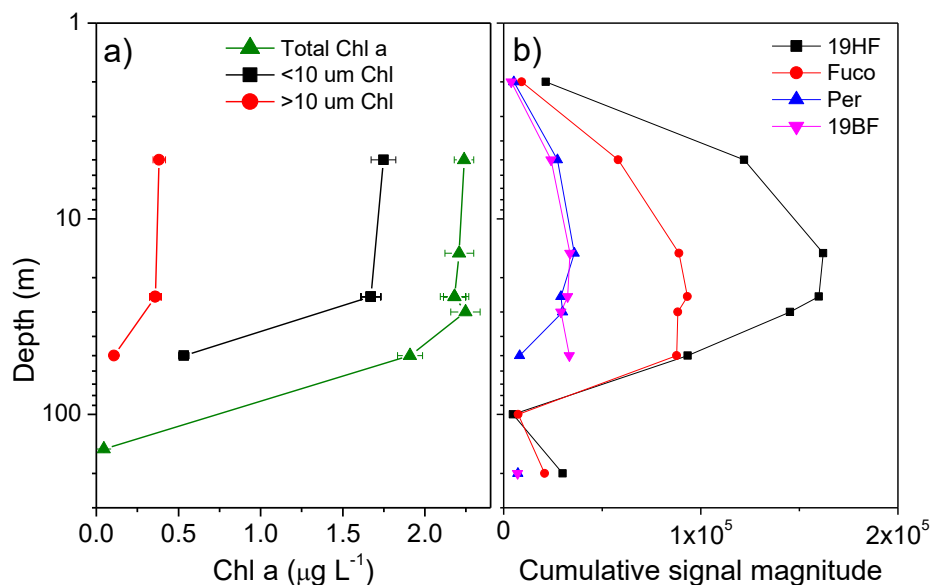
243

Pre-print version



245 Fig. 2. Depth distributions at PAP station of a) temperature, b) salinity, c) nitrates, d) nitrites, e)
246 ammonium, f) orthophosphates, and g) orthosilicates during the subpolar Northeast Atlantic cruise (the
247 Porcupine Abyssal Plain) during the whole cruise period. Sampling for the lipid analysis was performed
248 on June 14th 2013.

Pre-print version



249

250 Fig. 3. Depth related (a) total Chl *a* and size-fractionated Chl *a* distributions and (b) changes of the pigment
251 FT-ICR MS cumulative signal magnitude of 19'-Hexanoyloxyfucoxanthin (19HF) (squares), Fucoxanthin
252 (Fuco), (circles), Peridinin (Peri) (triangles) and 19'-Butanoyloxyfucoxanthin (19BF) (down triangles).

253 Depth related distributions of chlorophyll *a* (Chl *a*) and other pigments observed in the whole
254 water column are shown in Fig. 3. Chl *a* shows the highest concentration at the first 50 m depth. Size-
255 fractionated Chl *a* measurements revealed that the highest contribution to the total Chl *a* derived from
256 nanophytoplankton (<10 μm fraction) (82%), whereas microphytoplankton (>10 μm fraction) only
257 contributed to about 18% of the total Chl *a*. A similar situation was observed at other times during the
258 cruise (data not shown).

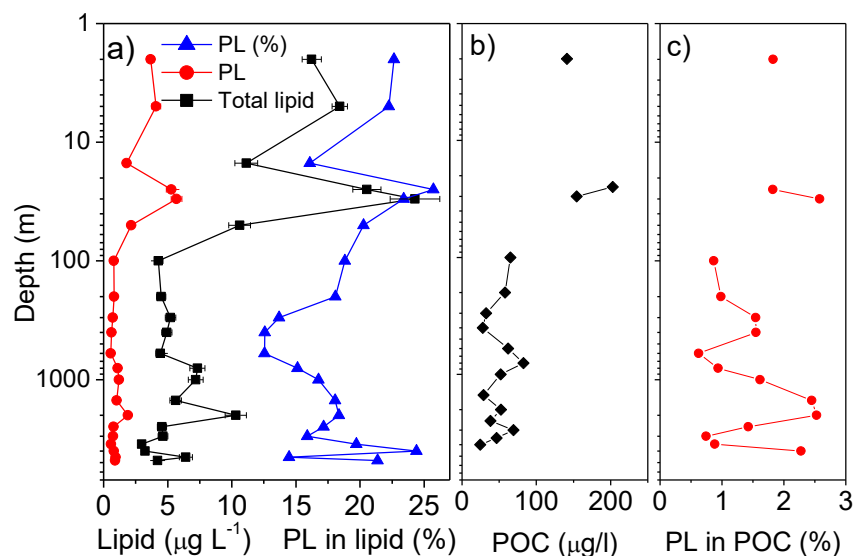
259 The FT-ICR MS data provide identification of the main phytoplankton pigments. 19'-
260 Hexanoyloxyfucoxanthin (19HF), Fucoxanthin (Fuco), Peridinin (Peri) and 19'-Butanoyloxyfucoxanthin
261 (19BF), shown in Fig. 3b, serve as markers for prymnesiophytes, diatoms, dinophyceae and chrysophytes,
262 respectively. The most abundant signals are observed for pigments that serve as markers for
263 prymnesiophytes (nanophytoplankton) and for diatoms (microphytoplankton).

264 We quantified total particulate lipids and phospholipids (PL) by Iatroscan-TLC-FID (Fig. 4a). This
265 technique provides information on total lipid content close to true gravimetric values (Parrish, 1987),
266 which are important for lipid mass balance calculation. Total lipids ranged from 3.0 to 24.3 $\mu\text{g L}^{-1}$. The
267 average decrease in total lipid content between the epipelagic and the abyssopelagic was 64%. The highest

Pre-print version

268 decrease was observed between the epipelagic and the mesopelagic. The Iatroscan TLC-FID technique
269 detected 3 classes of phospholipids: PG, PC, and PE, which are summed and reported as PL. There is no
270 protocol to detect phosphatidic acid (PA), phosphatidyl serine (PS) and phosphatidylinositol (PI) by
271 Iatroscan TLC-FID. However, PS and PA co-elute with PG, while PI co-elute with PC. PL varied between
272 $5.7 \mu\text{g L}^{-1}$ at 30 m depth and $0.6 \mu\text{g L}^{-1}$ at 3500 m depth. The decrease in PL between the epipelagic and
273 the abyssopelagic is 77%. The PL contribution to total lipids was highest in the epipelagic and the lowest
274 in the mesopelagic. The highest contribution was measured for the 30 m depth (25.7%) and the lowest for
275 the 400 m depth (12.6%).

276 The water column POC profile shows surface POC enrichment (up to $202.3 \mu\text{g L}^{-1}$) and a decrease
277 in concentration with depth (down to $24.3 \mu\text{g L}^{-1}$) (Fig. 4b). We do not have POC data for the whole water
278 column due to the irreparable damage to the samples during preparation. The contribution of PL to POC
279 range from 0.63 to 2.58% with an average of 1.54% (Fig. 4c).



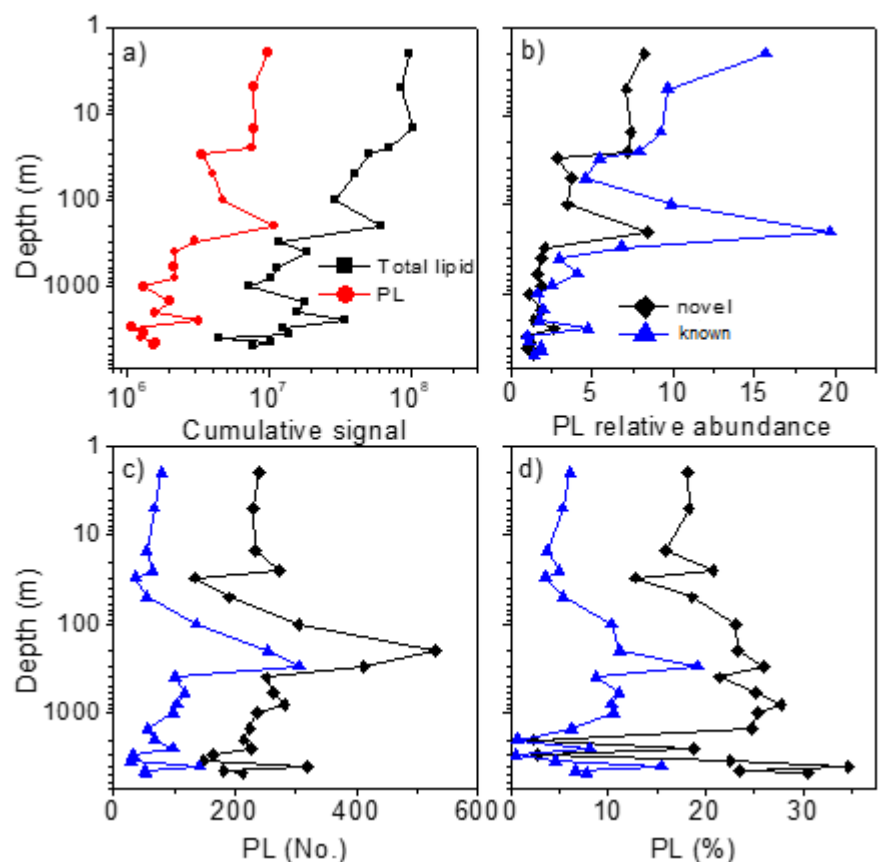
280

281 Fig. 4. Depth distribution of Iatroscan determined (a) total particulate lipids (squares), phospholipids (PL)
282 (circles), and the % contribution of PL to total lipids (triangles) and (b) POC and (c) the % contribution
283 of PL to POC.

284 The principal drawback of Iatroscan TLC/FID is its inability to resolve individual molecular
285 compounds in complex samples, thus providing only limited information on the sample composition.
286 Therefore, we performed direct infusion high resolution FT-ICR mass spectrometry to provide a detailed
287 molecular-level compositional description of the samples. High mass accuracy and mass resolving power

Pre-print version

288 in combination with Kendrick mass sorting enable unambiguous determination of elemental composition
289 for ~5,000 individual lipid compounds present in this sample set for negative ions and >8,500 compounds
290 between both ion polarities.



291

292 Fig. 5. Depth distribution of FT-ICR MS-determined (a) Total particulate lipid (squares), phospholipid
293 (PL) (circles) cumulative signal magnitude, (b) relative abundance of known (triangles) and novel
294 (diamonds) monoisotopic PL (c) the number of known (triangles) and novel (diamonds) monoisotopic PL
295 peaks and (b) the contribution of number of known (triangles) and novel (diamonds) PL to total number
296 of detected lipids.

297

298 The depth-dependent cumulative FT-ICR MS signal for total lipids and PL follow that of Iatroscan
299 TLC-FID technique, indicating that although FT-ICR MS method is not quantitative it does provide semi-
300 quantitative observation of bulk lipid content with depth. The cumulative signal of all lipids in negative
301 ionization mode decreased by 89% between the epipelagic and the abyssopelagic zones, while the PL
302 cumulative signal declined by 78% (Fig. 5a).

Pre-print version

303 We have identified 4,908 monoisotopic compounds (i.e., contribution from ^{13}C -containing species
304 and other heavy nuclides are omitted) for the negative ionization sample set. In total, elemental
305 compositions were assigned for 1,862 phosphorus-containing species (38%) of which only ~27% have
306 elemental compositions that match the database of known lipids. These novel P-containing lipids include
307 both compounds that are in continuous DBE and carbon-number series as known lipids (i.e. same
308 headgroup with more/less double bonds and or more/less acyl carbons than has been previously observed)
309 as well as compounds that do not have previously reported structures. The relative abundance of known
310 and novel PL shows a 5.1- and 4.7-fold decrease, respectively, from epipelagic to bathypelagic depths
311 (Fig. 5b). We observed no significant trend in the number of known and novel PL between the surface
312 and deep Atlantic (Fig. 5c), with a significantly higher diversity of PL at 200 and 300 m depth. The average
313 number of known and novel PL per depth is 95 and 251, respectively. The diversity of known and novel
314 PL molecules is higher at abyssopelagic depths (9.9% and 29.6% of all lipids, respectively) than in the
315 epipelagic (4.8% and 17.4% of all lipids, respectively).

316 Known PL include phosphatidylglycerol (PG), phosphatidylcholine (PC),
317 phosphatidylethanolamine (PE), phosphatidic acid (PA), phosphatidyl serine (PS), and
318 phosphatidylinositol (PI) that was occasionally detected at some depths (Fig. 6). Oxidized and monoacyl
319 forms are assigned but their contribution to the total PL signal was mainly below 0.1% for all depths and
320 is not discussed further. Isomeric PC and PE are differentiated as ions of different polarity (PC is observed
321 as a positively-charged ion and PE as a negatively-charged ion).

322 The relative abundance of known PL decreased with depth (Fig. 6a,e,i,m,r, and w). Among those
323 PL, the relative abundance decreased in the order $\text{PG} < \text{PE} < \text{PA} < \text{PC} < \text{PS} < \text{PI}$ from the epipelagic to the
324 abyssopelagic zone. Molecular diversity of these lipids is reflected in 82 PG, 39 PC, 22 PE, 92 PA, 28 PS
325 and 10 PI compounds detected. The water column distributions of their molecular diversities, *i.e.* the
326 number of detected PL are shown in Figs. 6 b,f,j,n,s,and x. There is an increased diversity of PG and PA
327 with depth (on average 15 PG and 12 PA formulas in the epipelagic, and 27 PG and 17 PA formulas in
328 the abyssopelagic). In contrast, molecular diversity of PC and PE decreased between the epipelagic (12
329 PC and 11 PE formulas) and abyssopelagic (5 PC and 4 PE formulas). Their contribution to all lipid
330 molecules increased down to the deep Atlantic for PG and PA, from the average of 1.2% and 1.0%
331 respectively, in the epipelagic layer, to the average of 3.4% and 2.1% respectively, in the abyssopelagic

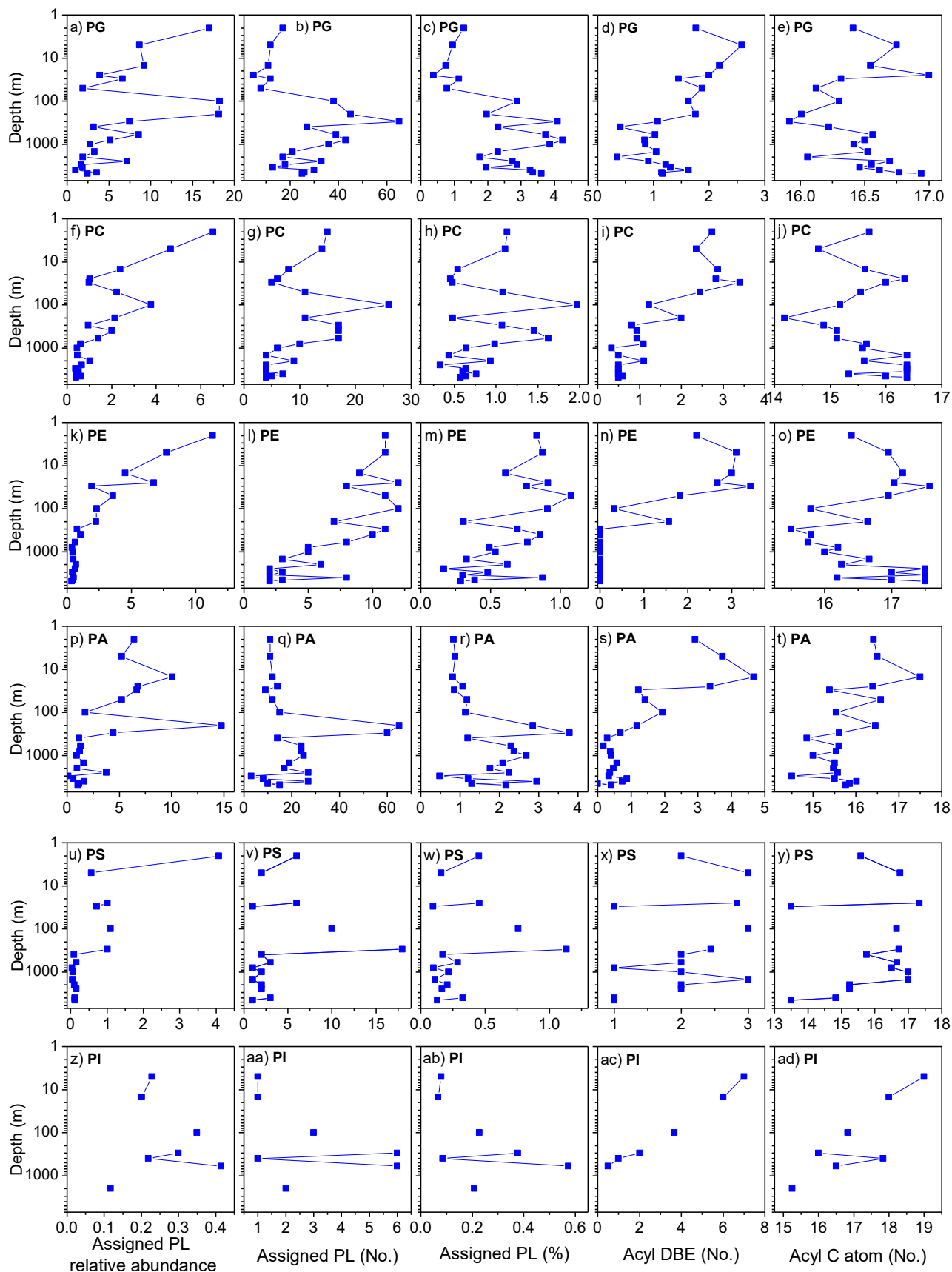
Pre-print version

332 layer. The contribution of PC, PE, PS and PI to all lipid molecules slightly decreased to less than 1% in
333 the deep Atlantic

334 The acyl double bond equivalents (DBE, the number of molecular rings plus double bonds to
335 carbon in a molecule) and the acyl chain length facilitate insight into the structural characteristics of
336 identified PL. Average DBE (Fig. 6d,h,l,p,u and z) decreased from surface to the deep ocean for all 6
337 identified PL. Detected PE were saturated below 200 m depth. The highest unsaturation in the epipelagic
338 zone was observed for a few detected PI (average DBE=5.6), while the lowest unsaturation at the surface
339 was observed for PG (average DBE=1.9). The average number of carbon atoms in acyl chain (Fig.
340 6d,h,l,p,u and z) across ocean depths varies for PG (between 15.9 and 17.0 C atoms), for PC (between
341 14.2 and 16.4 C atoms), for PE (between 15.5 and 17.6 C atoms), for PA (between 14.5 and 17.5 C atoms),
342 for PS (between 13.5 and 17.3 C atoms) and for PI (between 15.3 and 19.0 C atoms). This highlights an
343 elongation in the PG, PC and PE acyl carbon chain in the abyssopelagic zone.

344

Pre-print version



Pre-print version

346 Fig. 6. Depth distribution of FT-ICR MS determined known phospholipids (PL): (a, f, k, p, u and z) PL
 347 relative abundance, (b, g, l, q, v and aa) the number of monoisotopic peaks, (c, h, m, r, w and ab) the
 348 contribution of PL molecular number to total number of detected lipids, (d, i, n, s, x, and ac) acyl double
 349 bond equivalents and (e, j, o, t, y and ad) acyl carbon number of (a-e) phosphatidylglycerol (PG), (f-j)
 350 phosphatidylcholine (PC), (k-o) phosphatidylethanolamine (PE), (p-t) phosphatidic acid (PA), (u-y)
 351 phosphatidyl serine (PS), and (z-ad) phosphatidylinositol (PI).

352

353 We have observed that some PL dominate in the epipelagic (0-100 m depth), or below the
 354 epipelagic to the abyssopelagic (100-4800 m depth). Table 1 shows acyl DBE (for known PL), molecular
 355 DBE (for novel PL) and carbon number of the most abundant (assuming similar ionization efficiency
 356 between PL) known lipids observed in the epipelagic and below the epipelagic and their contribution to
 357 the total known lipid class as well as to the total novel lipids.

358

359 Table 1. The elemental composition, average carbon number and double bond equivalents (DBE) of the
 360 acyl group, and their contribution to the lipid class, range and average value (in parentheses), for the most
 361 abundant lipids observed in the epipelagic (0-100 m) and below the epipelagic (100-4800 m). The formula
 362 in bold represents the most abundant lipid compound observed in the whole water column.

363

	Elemental composition	Average acyl DBE	Average acyl C number	Contribution to the lipid class (%)	Elemental composition	Average acyl DBE	Average acyl C number	Contribution to the lipid class (%)
	0-100 m				100-4800 m			
a) Known								
PG	$C_{38}H_{70}O_{10}P_1$	2	16	27-68 (47)	$C_{38}H_{72}O_{10}P_1$	1	16	6-40 (24)
	$C_{40}H_{74}O_{10}P_1$	2	17		$C_{40}H_{74}O_{10}P_1$	2	17	
PC	$C_{39}H_{71}N_1O_8P_1$	3	16.5	28-45 (35)				
	$C_{40}H_{75}N_1O_7P_1$	3	17					
PE				38-49 (43)				
	$C_{39}H_{71}N_1O_7P_1$	3	16.5					
b) Novel								
	Elemental composition	DBE		%	Elemental composition	DBE		%

Pre-print version

DBE>0	C ₃₉ H ₇₁ N ₁ O ₅ P ₁ C ₃₆ H ₆₇ N ₁ O ₅ P ₁	5 4		6-12 (9)	C ₂₈ H ₄₂ O ₄ P ₁	8		2-6 (8)
DBE=0	C ₃₃ H ₆₈ O ₇ P ₁ C ₃₁ H ₆₄ O ₇ P ₁	0 0		1-3 (2)	C ₂₀ H ₄₂ O ₆ P ₁ C ₂₂ H ₄₆ O ₆ P ₁	0 0		1-5 (2)

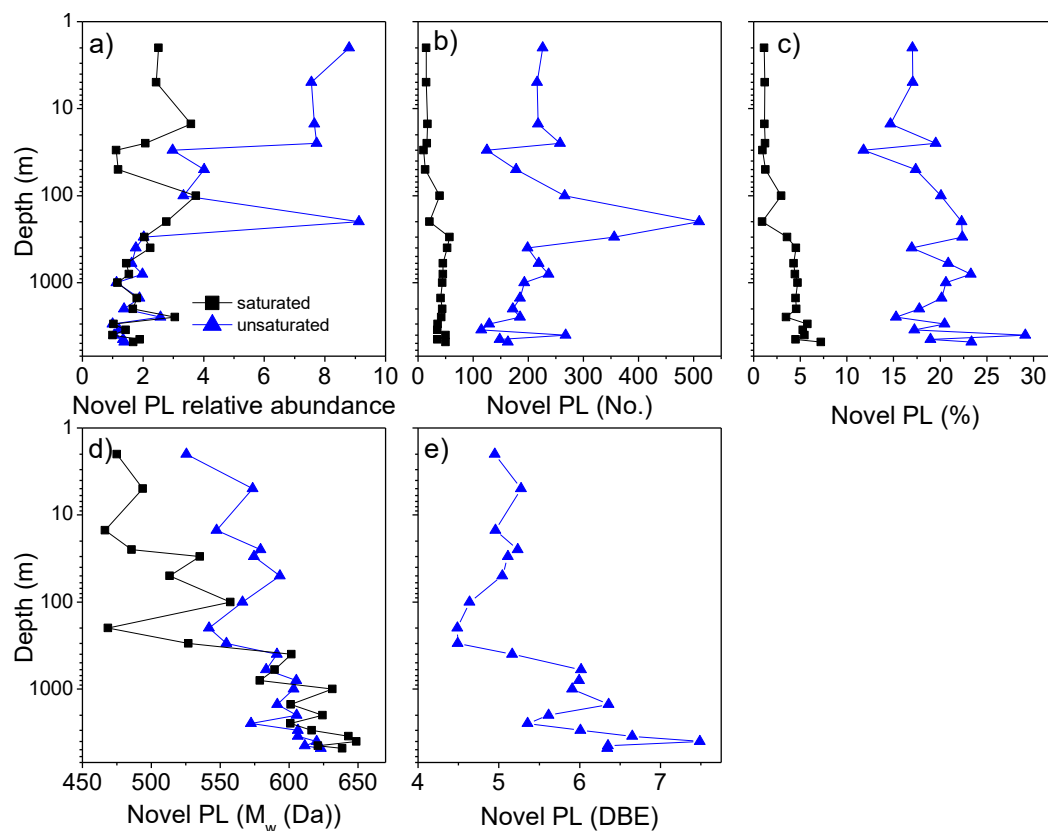
364

365 To provide insight into the chemical characteristics of novel PL, we have categorized them into
 366 two groups; novel PL with at least one unsaturation (DBE>0) and saturated (DBE=0) novel PL. The
 367 relative abundance of unsaturated novel PL decreased 5.0-fold, while for saturated PL relative abundance
 368 decreased 1.6-fold between the epipelagic and the abyssopelagic layers (Fig. 7a). The highest relative
 369 abundance decrease for unsaturated novel PL was observed between the epipelagic and the mesopelagic
 370 zones.

371 The number of novel saturated molecular formulae (Fig. 7b) increased from epipelagic (on average
 372 18) to the abyssopelagic (average 45), with an increased contribution to total lipid diversity. Molecular
 373 diversity increased from an average 1.2% at the surface productive layer to 5.7% at the deepest Atlantic
 374 (Fig. 7c). The change in the number of unsaturated novel PL between the surface (on average 203
 375 molecules) and deep ocean (average 192 molecules) is not significant, but a substantial increase was
 376 noticed in the mesopelagic layer (Fig. 7b). The contribution of novel unsaturated PL molecular formulas
 377 to total lipid molecular formulae increased between the epipelagic and the abyssopelagic zone from 16.2
 378 to 23.8% (Fig. 7c). The molecular mass (Fig. 7d) of saturated and unsaturated novel PL increased with
 379 depth. For example, average molecular weight for saturated novel PL increased from 466.5 Da (at the
 380 surface) to 648.7 Da (at 4800 m), whereas unsaturated PL showed an increase from 524.5 Da (at the
 381 surface) to 623.1 Da (at 4800 m). Interestingly, we observe a depth-related increase in the degree of
 382 unsaturation of novel unsaturated PL from an average DBE value of 5.0 in the epipelagic to 6.7 in the
 383 abyssopelagic (Fig. 7e).

384

Pre-print version



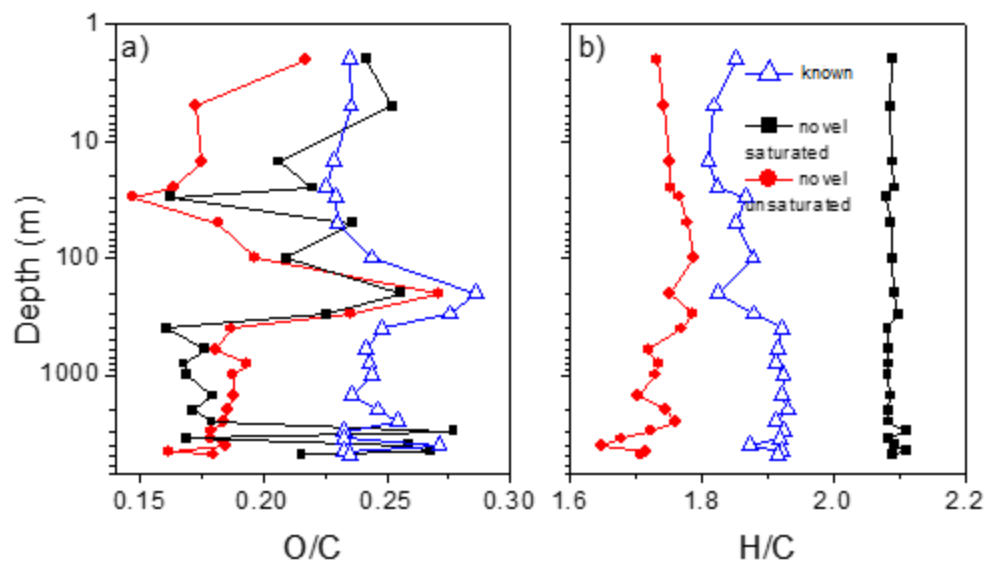
385

386 Fig. 7. Depth distribution of FT-ICR MS determined novel phospholipids: (a) relative abundance, (b) the
387 number of monoisotopic peaks (No.), (c) the contribution of PL molecular formulas to total lipid molecular
388 formulas (%), (d) the average molecular weight and (e) double bond equivalents (DBE) for saturated
389 (squares) and unsaturated (triangles) PL.

390 It is reasonable to assume that the majority of novel PL are products of depth related transformation
391 of PL. Here we present depth-related average oxygen to carbon (O/C) and hydrogen to carbon (H/C) ratio
392 variations of elaborated PL classes obtained in the negative ionization mode, with the intention to gain
393 insight into the possible transformation mechanisms of PL in the whole water column. The average O/C
394 ratio (Fig. 8a) varied more with depth than H/C ratios (Fig. 8b). The highest O/C was recorded for known
395 PL (on average 0.24), and declined for saturated (on average 0.21) and unsaturated (on average 0.19)
396 novel PL. PL characteristic is their richness in hydrogen and the H/C ratios were on average 1.89, 1.74
397 and 2.09 for the known, novel unsaturated and novel saturated PL, respectively (Fig. 8b).

398

Pre-print version



399

400 Fig. 8. Depth related FT-ICR MS data of (a) average oxygen to carbon (O/C) and (b) hydrogen to carbon
401 (H/C) ratios of known PL (triangles), novel unsaturated PL (circles) and novel saturated PL (squares).

402

403 **Discussion**

404

405 Here, we have analyzed PL and identify them as known (database-matched) and novel. Known
406 phospholipids, PG, PC, PE, PA, PS and PI, are discussed individually, while novel PL are analyzed and
407 discussed as saturated (DBE=0) and unsaturated, having one or more double bonds (DBE>0). This
408 approach provides a holistic assesment of PL in the Northeast Atlantic, in which the change in both relative
409 abundance and composition occur most significantly in the upper regions of the water colum while PL are
410 sinking to 4800 m depth in the Northeast Atlantic.

411 Lipids, like bulk POC, are produced primarily in surface waters by plankton and are largely
412 recycled and degraded in sub-surface waters (Gašparović et al., 2014; Wakeham, 1995). Size-fractionated
413 Chl *a* measurements and pigment analysis revealed that the main lipid producers were nanophytoplankton
414 prymnesiophytes and microphytoplankton diatoms. Although microphytoplankton contributed less to the
415 total Chl *a* it seems that diatom bloom resulted in SiO_4^{4-} depletion in the first 50 m of the water column.
416 Judging from the PO_4^{3-} concentrations it was not a limiting nutrient, knowing that PO_4^{3-} threshold values
417 for the phytoplankton uptake is $0.1 \mu\text{mol l}^{-1}$ (Justić et al., 1995).

418 The most significant output of phosphorus from the oceans is in organic debris sinking to the ocean
419 floor and becoming incorporated into sedimentary rocks (Tyrell, 1999). The sinking particulate P pool
420 (e.g., collected in sediment traps) is composed of particulate organic P (POP) (~40%), authigenic
421 particulate inorganic P (PIP) (~25%), which is formed when organic P is remineralized and reprecipitated
422 as calcium fluorapatite, and labile PIP (21%), with lesser amounts of nonreactive detrital P (~13%) (Faul
423 et al., 2005). In order to understand oceanic cycles of phosphorus and carbon, it is important to gain an
424 insight into lipids that contribute to POP, as well as to POC, especially in the light of lipid selective
425 accumulation in the ocean water column as POC sinks (Hwang and Druffel, 2003). As there are many
426 unanswered questions regarding the global phosphorus cycle (Paytan and McLaughlin, 2007) we believe
427 that our research will provide a means to better understand the P cycling in the ocean and the capability
428 of PL for carbon sequestration.

429 Although total lipid and PL concentration, determined by the Iatroscan TLC/FID technique,
430 decreased with depth, we observed that PL contribute to a significant fraction of POC (1.54%) in the water

Pre-print version

431 column together with other lipid classes and a variety of other molecules that contribute to POC in the
432 oceans.

433 The depth-related relative abundance distribution of known PL indicate their production at the
434 surface layer and recycling in deeper layers. We note that the contribution of PG and PA (Fig. 6c and o),
435 together with novel saturated and unsaturated PL (Fig. 7.c) to all identified lipid molecules increased with
436 depth, which indicated that those PL are selectively preserved among other lipid classes during particle
437 sinking. Paytan et al. (2003) found that in a wide range of oceanic regimes a significant fraction of organic
438 P (which includes PL) is exported to depths below the euphotic zone, although preferential regeneration
439 of P relative to C occurs predominantly at shallow depths in the water column, but not deeper (>300 m)
440 (Faul et al., 2005). There are several possible explanations for depth-related PL preservation. One means
441 is the export by faecal pellets, which are shown to be rich in P and in which solubilization of P is prevented
442 (Temelender et al., 2012). High pellet sedimentation rate should also contribute to P export from the
443 epipelagic. Furthermore, Yoshimura et al. (2009) suggested that structural lipids (membrane compounds
444 such as PL) remain stable during early lipid transformation due to the chemical interactions of the
445 structural lipids with other organics. Depth-related enhanced contribution of PL molecules to all lipid
446 molecules can also be explained by efficient particle export during diatom and coccolithophorides
447 (Prymnesiophyceae) blooms. In general, diatom blooms can lead to substantial particle export that is
448 transferred efficiently through the mesopelagic (Martin et al., 2011b). Coccolithophores, class
449 Prymnesiophyceae, calcifying marine phytoplankton, are shown to bloom frequently and extensively in
450 the North Atlantic (Brown and Yoder, 1994). They are considered to play an important role in the global
451 carbon cycle through the production and export of organic carbon and calcite (O'Brien et al., 2013).

452 The major PL in many species of algae are PC, PE and PG. In addition, PS may also be found in
453 substantial amounts. PI and PA are noted as minor compounds (Guschina and Harwood, 2009). PA is an
454 essential phospholipid involved in membrane biosynthesis and signal transduction in all eukaryotes
455 (Testerink and Munnik, 2011). In this work we assigned a variety of PG, PE, PC, PA, PS and PI molecules.
456 Among them the most abundant with the highest molecular diversity were PG. Obviously PG were major
457 plankton membrane forming lipids at PAP site. Although the relative abundance of all known PL decreases
458 with depth, due to heterotrophic consumers that selectively degrade and alter PL, abiotic transformations,
459 and a substantial decrease of life below the euphotic zone, they are preserved to a different degree across

Pre-print version

460 the water column. PG and PA are selectively preserved. We may eventually assume that those PL
461 originated from fast settling particles coming from diatoms and prymnesiophytes. However, we are unable
462 to explain the depth-related increased molecular variability of PG. It seems that a new source of PG
463 contributed to PG diversity at 300 m depth. This could be due to the horizontal advection of water masses,
464 transportation of old particles to the deep waters that were previously produced in the euphotic zone and/or
465 newly produced prokaryotic biomass *in-situ* below euphotic zone.

466 We found PA as an important component of PL pool regarding high molecular diversity (Fig. 6.).
467 We assume that PA can also be formed *in-situ* during the early transformation of PL. We propose two
468 possible mechanisms that generate PA from other PL: nucleophilic substitution of the P atom enabled by
469 abiotic hydrolysis or biotic enzymatic reaction with cleavage of glycerol, choline, ethanolamine, serine
470 and inositol from PG, PC, PE, PS and PI, respectively.

471 Higher average unsaturation of known PL at the surface indicates their primary origin from
472 plankton. Their depth related characteristics include loss of unsaturation. It is clear that saturated lipids
473 are less prone to degradation and are therefore important organics for deep ocean carbon storage. It is not
474 clear what would be the origin of PG, PC and PE acyl chain elongation in the abyssopelagic. One possible
475 explanation would be that the majority of those lipids came from living cells and represent their
476 acclimation to low temperature and high pressure, a feature that should be explored.

477 We have found that two PGs dominated in the surface productive layer (Table 1a). PG
478 $C_{38}H_{70}O_{10}P_1$, with acyl DBE=2 and an average acyl carbon number of 16 C per acyl chain, for which we
479 assume that these acyl chains might be two 16:l(n-7) fatty acids, which is a marker for diatoms (Daalgstad
480 et al., 2003). It is reasonable to assume that as we have found a strong signal of the diatom pigment
481 Fucoxanthin in the epipelagic layer (Fig. 3). PG $C_{40}H_{74}O_{10}P_1$, with DBE=2 and an average acyl carbon
482 number of 17 C per acyl chain, was found to be dominant in the whole water column (Table 1a) indicating
483 it as an important marker, probably of some living plankton origin. We anticipate two fatty acids 16:0 and
484 18:2(n-6), which are common for Prymnesiophyceae, for which the pigment 19HF was found to be the
485 most abundant in our samples (Fig. 3). If it is so, then, we may conclude that a Prymnesiophyceae bloom
486 was the cause of export of organic carbon and phosphorus. The average 16.5 carbons in the acyl chain of
487 PC $C_{39}H_{71}N_1O_8P_1$ and PE $C_{39}H_{71}N_1O_7P_1$ indicate that one of two fatty acids have an odd number of C
488 atoms. An odd number of fatty acid C atoms point to PL of bacterial origin (Harkewicz and Dennis, 2011).

Pre-print version

489 We find a predominance of novel PL molecules in the North Atlantic samples that constituted an
490 increasing molecular contribution to total lipid molecules detected. This implies their depth-related
491 selective accumulation. Suzumura and Ingall (2004) found similar results while investigating different P
492 forms, including hydrophobic P (representing phospholipids) in the Pacific Ocean. They found that a
493 fraction of the hydrophobic P is less reactive that withstands recycling in surface waters and is exported
494 to deeper waters. In deep water preferential remineralization of non-hydrophobic compounds results in an
495 increased abundance of hydrophobic P in both dissolved and particulate OM fractions relative to surface
496 waters. They concluded that accumulation of less reactive hydrophobic P compounds in deep waters acts
497 as a P sink from the marine ecosystems on a longer time scale.

498 Obviously, there is a lack of knowledge on the molecular form of phosphorus stored in lipids,
499 production of those PL, and depth related molecular changes. Further research should be focused on those
500 PL molecular identification to further elucidate oceanic P cycling. These PL are primarily non-aromatic
501 in their molecular structure as illustrated from the Aromaticity Index (AI) (Koch and Dittmar, 2006) that
502 is mainly <0.5 for the majority of novel lipids. We have found 1-4 molecular PL formulas per depth that
503 satisfy the criteria for the existence of aromatic structures ($AI > 0.5$). For example, the two most often
504 found PL formulas having $AI > 0.5$ at a majority of depths are $C_{28}H_{24}O_2P_1$ (DBE=17, $AI=0.56$) and
505 $C_{29}H_{22}N_1O_2S_1$ (DBE=19, $AI=0.60$).

506 The degree of unsaturation of the novel unsaturated PL at the surface was quite high (average
507 DBE=5) and even higher than the majority of known PL with the exception of PI. We assume that the
508 majority of those PL represent the first stage of PL degradation concluding from the fact that they are still
509 isolated as a lipid fraction by the use of dichloromethane. However, we cannot ignore the possible
510 contribution of *in-situ* biologically produced intact PL to novel PL, whose formulae and biological
511 function so far are not know. A remarkable observation is an increase in the degree of unsaturation in the
512 deep ocean (abyssopelagic average DBE=6.7). This degree of unsaturation is not easily explainable as PL
513 transformation during particle sinking, because unsaturated organic compounds are generally considered
514 as more reactive than saturated organics. One explanation would be that during PL transformation, cross-
515 linking of unsaturated PL with other unsaturated organics or their fragments take place. This agrees with
516 the findings of Yoshimura et al. (2009) that membrane compounds chemically interact with other organics.
517 These processes would lead to the formation of molecules with higher unsaturation and consequently

Pre-print version

518 higher molecular sizes, as we observed (Fig. 7e). Another explanation would be that some proportion of
519 those highly unsaturated PL might arise from deep ocean plankton, such as bacteria, and to a much lesser
520 degree from protozooplankton, and mesozooplankton (Yamaguchi et al., 2002). De Carvalho and
521 Caramujo (2012) have shown that deep ocean bacteria are able to produce polyunsaturated fatty acids
522 helping the regulation of the membrane fluidity triggered by low temperature and high pressure and
523 providing protection from oxidative stress. If there were plankton membrane PL among novel unsaturated
524 lipids in the deep ocean they should contain elongated highly unsaturated fatty acids judging from the
525 high increased molecular mass.

526 The relative abundance of novel saturated PL slightly decreased with depth, with an increased
527 molecular contribution to the total lipid molecular number with depth. This suggest that during particle
528 sinking PL chemical transformations lead to *in-situ* formation of new saturated PL compounds and this is
529 in line with their depth related increased molecular diversity and molecular mass. Four dominant novel
530 saturated PL (Table 1) are probably important PL transformation products.

531 We assume that most novel unsaturated and saturated PL are formed during the transformation of
532 PL. Molecular transformation of lipids takes place by biotic (enzymatic peroxidation, biohydrogenated
533 (Rontani and Koblížek, 2008)) and abiotic (photooxidation and autoxidation) degradation (Rontani, 2008).
534 However, the chemical mechanisms of these processes are largely unknown at present. Photooxidation
535 can be important within the euphotic layer, whereas autoxidation and biotransformation may occur
536 throughout the water column (Rontani et al., 2009). Biotic (heterotrophic) degradation was important for
537 sinking particles and increased with depth, whereas abiotic degradation dominated the suspended particle
538 pool (Christodoulou et al. 2009). Harvey et al. (1995) have shown that oxygen has a substantial effect on
539 the overall rates of decomposition of lipid and other major biochemical compounds. The fact that O/C
540 ratios of novel saturated and unsaturated PL are lower than O/C ratios of intact known PL implies that
541 oxidative transformation of PL does not take a leading role in PL transformation. In fact, decreased oxygen
542 content in all novel PI indicates oxygen removal from the molecules. Judging from the decreased H/C
543 ratio of novel unsaturated PL it seems that dehydrogenation is an important mechanism in their formation.
544 Conversely, hydrogenation is important for the formation of novel saturated PL. Marine bacteria and fungi
545 were shown to perform biohydrogenation (Rhead et al., 1971; Wakeham, 1989; Ferreira et al., 2015).

546

547

548 **Conclusions**

549 Phosphorus cycling within the ocean is not well understood (Benitez-Nelson, 2000). Much remains
550 to be determined regarding the distribution, composition, and spatial and temporal variability of particulate
551 phosphorus. Chemical characterization of lipids in particulate organic matter (POM) is necessary not only
552 for understanding the source but also for clarifying the mechanistic processes by which PL survive across
553 ocean depths.

554 The application of high-resolution FT-ICR MS provided a detailed compositional overview of
555 particulate PL in the Northeast Atlantic including elemental composition, saturation/unsaturation,
556 molecular mass and H/C and O/C ratios that illustrates depth-related transformation mechanisms of PL.
557 Apart from the known PL that derive from living plankton or fresh OM, we primarily observed saturated
558 and unsaturated PL that have not been reported previously. We have shown that novel PL are selectively
559 preserved among other lipid classes and are a vehicle for the transportation of phosphorus as well as for
560 carbon to the deep ocean. Further focus should be applied to their in-depth molecular identification and
561 resolving their possible ecological functions.

562 Major pathway of known PL (PG, PC, PE, PA, PS and PI) cycling includes depth related loss of
563 unsaturation, with PA formed as the earliest transformation of PG, PC, PE, PS and PI. We assume that
564 novel, more resistant to transformation, PL originate from known PL alteration, for which oxidative
565 transformation is not an important transformation mechanism.

566 This work provide new light in the P cycling in lipids, molecular diversity as well as the depth
567 related PL molecular changes.

568

569 **Acknowledgements** We thank crew of the RRS James Cook. We would like to thank Gayatri Dudeja
570 and Zoe Morral for the pigment and POC sample collection and analysis. This work was funded by the
571 grant from the Croatian Science Foundation under the project IP-11-2013-8607, by the United States
572 National Science Foundation (IIA-1301346) and the Center for Animal Health and Food Safety at New
573 Mexico State University. This work is a contribution of the European FP7 Projects EURO-BASIN and of
574 the Natural Environment Research Council, UK, core programme.

Gašparović, B., Penezić, A., Lampitt, R.S., Sudasinghe, N., Schaub, T. 2018. Phospholipids as a component of the oceanic phosphorus cycle. *Mar. Chem.* 250, 70-80.

Pre-print version

575

Gašparović, B., Penezić, A., Lampitt, R.S., Sudasinghe, N., Schaub, T. 2018. Phospholipids as a component of the oceanic phosphorus cycle. *Mar. Chem.* 250, 70-80.

Pre-print version

576 **References**

- 577 Azam, F., 1998. Microbial control of oceanic carbon flux: the plot thickens. *Science* 280, 694–696.
- 578 Baturin, G.N., 2003. Phosphorus Cycle in the Ocean, *Lithology and Mineral Resources*, 38, 101–119.
- 579 Benitez–Nelson, C.R., 2000. The biogeochemical cycling of phosphorus in marine systems. *Earth–Sci.*
580 *Rev.* 51, 109–135.
- 581 Blight, E.G., Dyer, W.J., 1959. A rapid method of total lipid extraction and purification. *Can. J. Biochem.*
582 *Physiol.* 37, 911–917.
- 583 Brown, C., Yoder, J., 1994. Coccolithophorid blooms in the global ocean, *J. Geophys. Res.*, 99, 7467–
584 7482.
- 585 Buesseler, K.O., 1998. The decoupling of production and particulate export in the surface ocean. *Global*
586 *Biogeochem. Cycles* 12, 297–310.
- 587 de Carvalho, C.C.C.R., Caramujo, M.J., 2012. Lipids of Prokaryotic Origin at the Base of Marine Food
588 *Webs. Mar. Drugs* 10, 2698–2714.
- 589 Chelton, D.B., Schlax, M.G., Samelson, R.M., de Szoeko, R.A., 2007. Global observations of large
590 oceanic eddies. *Geophys. Res. Letters* 0094-8276. 34 (15) p:L15606.
- 591 Christodoulou, S., Marty, J.C., Miquel, J.C., Volkman, J.K., Rontani, J.F., 2009. Use of lipids and their
592 degradation products as biomarkers for carbon cycling in the northwestern Mediterranean Sea.
593 *Marine Chemistry* 113, 25-40.
- 594 Dalsgaard, J., St John, M., Kattner, G., Müller–Navarra, D., Hagen, W., 2003. Fatty acid trophic markers
595 in the pelagic marine environment. *Adv. Mar. Biol.* 46, 225–340.
- 596 Dobbs, F.C., Findlay, R.H., 1993. Analysis of microbial lipids to determine biomass and detect the
597 response of sedimentary microorganisms to disturbance. In: Kemp, P.F., Sherr, B.F., Sherr, E.B.,
598 Cole, J.J. (Eds.), *Handbook of Methods in Aquatic Microbial Ecology*. Lewis Publisher, Boca
599 Raton, FL, pp. 347–358.
- 600 Dugdale, R.C., Goering, J.J. 1967. Uptake of new and regenerated forms of nitrogen in primary
601 productivity. *Limnol. Oceanogr.* 12, 196-206.

Gašparović, B., Penezić, A., Lampitt, R.S., Sudasinghe, N., Schaub, T. 2018. Phospholipids as a component of the oceanic phosphorus cycle. *Mar. Chem.* 250, 70-80.

Pre-print version

- 602 Faul, K.L., Paytan, A., Delaney, M.L. 2005. Phosphorus distribution in sinking oceanic particulate matter.
603 *Mar. Chem.*, 97, 307–333.
- 604 Ferreira, I.M., Meira, E.B., Rosset, I.G., Porto, A.L.M., 2015. Chemoselective biohydrogenation of α,β -
605 and $\alpha,\beta,\gamma,\delta$ -unsaturated ketones by the marine-derived fungus *Penicillium citrinum* CBMAI 1186 in
606 a biphasic system. *J. Mol. Cat. B Enzym.* 115, 59–65.
- 607 Frka, S., Gašparović, B., Marić, D., Godrijan, J., Djakovac, T., Vojvodić, V., Dautović, J., Kozarac, Z.
608 2011. Phytoplankton Driven Distribution Of Dissolved And Particulate Lipids In A Semi-Enclosed
609 Temperate Sea (Mediterranean): Spring To Summer Situation. *Estuar. Coast. Shelf Sci.* 93, 290-304.
- 610 Gašparović, B., Frka, S., Koch, B.P., Zhu, Z.Y., Bracher, A., Lechtenfeld, O. J., Neogi, S.B., Lara, R.J.,
611 Kattner, G., 2014. Factors influencing particulate lipid production in the East Atlantic Ocean.
612 *Deep-Sea Res. Pt. I* 89, 56–67.
- 613 Gašparović, B., Kazazić, S.P., Cvitešić, A., Penezić, A., Frka, S. 2015. Improved separation and analysis
614 of glycolipids by Iatroscan thin-layer chromatography–flame ionization detection. *J. Chromtogr.*
615 *A* 1409, 259–267.
- 616 Gašparović, B., Kazazić, S.P., Cvitešić, A., Penezić, A., Frka, S., 2017. Corrigendum to “Improved
617 separation and analysis of glycolipids by Iatroscan thin-layer chromatography–flame ionization
618 detection” [*J. Chromatogr. A* 1409 (2015) 259–267]. *J. Chromtogr. A* 1521, 168–169.
- 619 Geider, R.J., La Roche, J., 2002. Redfield revisited: variability of C:N:P in marine microalgae and its
620 biochemical basis. *Eur. J. Phycol.* 37, 1–17.
- 621 Guschina I.A., Harwood J.L., 2009. Algal Lipids and Effect of the Environment on their Biochemistry.
622 In: Arts, M.T., Brett, M.T., Kainz, M.J. (Eds.) *Lipids in Aquatic Ecosystems*. Springer, pp 1–24.
- 623 Harkewicz, R.; Dennis, E.A. Applications of mass spectrometry to lipids and membranes. *Annu. Rev.*
624 *Biochem.* 2011, 80, 301–325.
- 625 Hartman, S.E., Larkin, K.E., Lampitt, R.S., Lankhorst, M., Hydes, D.J., 2010. Seasonal and inter-annual
626 biogeochemical variations in the Porcupine Abyssal Plain 2003–2005 associated with winter
627 mixing and surface circulation. *Deep-Sea Res. II* 57 (15), 1303–1312.

Gašparović, B., Penezić, A., Lampitt, R.S., Sudasinghe, N., Schaub, T. 2018. Phospholipids as a component of the oceanic phosphorus cycle. *Mar. Chem.* 250, 70-80.

Pre-print version

- 628 Hartman, S.E., Lampitt, R.S., Larkin, K.E., Pagnani, M., Campbell, J., et al., 2012. The Porcupine Abyssal
629 Plain fixed-point sustained observatory (PAP-SO): variations and trends from the Northeast
630 Atlantic fixed-point time-series. *ICES J. Mar. Sci.* 69, 776–783.
- 631 Harvey, H.R., Tuttle, J.H., Bell, J., 1995. Kinetics of phytoplankton decay during simulated sedimentation,
632 Changes in biochemical composition and microbial activity under oxic and anoxic conditions.
633 *Geochim. Cosmochim. Acta*, 59, 367–3377.
- 634 Holguin, F.O., Schaub, T., 2013. Characterization of microalgal lipid feedstock by direct-infusion FT-
635 ICR mass spectrometry. *Algal Res.* 2, 43–50.
- 636 Hwang, J., Druffel, E.R.M., 2003. Lipid-like material as the source of the uncharacterized organic carbon
637 in the ocean? *Science* 299, 881–884.
- 638 Ivančić, I., Godrijan, J., Pfannkuchen, M., Marić, D., Gašparović, B., et al., 2012. Survival mechanisms
639 of phytoplankton in conditions of stratification induced deprivation of orthophosphate: Northern
640 Adriatic case study. *Limnol. Oceanogr.* 57, 1721–1731.
- 641 Karl, D.M., 2014. Microbially mediated transformations of phosphorus in the sea: new views of an old
642 cycle. *Ann. Rev. Mar. Sci.* 6, 279–337.
- 643 Kirkwood, D. S. 1996. Nutrients: practical notes on their determination in seawater. ICES, Copenhagen,
644 pp 1–25.
- 645 Koch, B.P., Dittmar, T., 2006. From mass to structure: an aromaticity index for high-resolution mass data
646 of natural organic matter. *Rapid Comm. Mass Spectrom.* 20, 926–932.
- 647 Lampitt, R.S., Bett, B.J., Kiriakoulis, K., Popova, E.E., Ragueneau, O., Vangriesheim, A., Wolff, G.A.,
648 2001. Material supply to the abyssal seafloor in the Northeast Atlantic. *Prog. Oceanogr.* 50, 27–
649 63.
- 650 Lampitt, R.S., Achterberg, E.P., Anderson, T.R., Hughes, J.A., Iglesias-Rodríguez, M.D., et al., 2008.
651 Ocean fertilization: a potential means of geoengineering? *Phil. Trans. Roy. Soc. A* 366, 3919–
652 3945.
- 653 Lee C., Wakeham, S., Arnosti C., 2004. Particulate organic matter in the sea: the composition conundrum.
654 *Ambio*, 33, 565–575.

Gašparović, B., Penezić, A., Lampitt, R.S., Sudasinghe, N., Schaub, T. 2018. Phospholipids as a component of the oceanic phosphorus cycle. *Mar. Chem.* 250, 70-80.

Pre-print version

- 655 Loh, A.N., Bauer, J.E. 2000. Distribution, partitioning and fluxes of dissolved and particulate organic C,
656 N and P in the eastern North Pacific and Southern Oceans. *Deep-Sea Res.*, I 47, 2287–2316.
- 657 Longhurst, A., 2007. *Ecological Geography of the Sea*, 2nd Ed. Academic Press, Amsterdam, p. 157–163.
- 658 Marić, D., Frka, S., Godrijan, J., Tomažić, I., Penezić, A., Djakovac, T., Vojvodić, V., Precali, R.,
659 Gašparović, B. 2013. Organic matter production during late summer-winter period in a temperate sea.
660 *Cont. Shelf Res.* 55, 52–65.
- 661 Martin, P., Van Mooy, B.A.S., Heithoff, A., Dyhrman, S.T., 2011a. Phosphorus supply drives rapid
662 turnover of membrane phospholipids in the diatom *Thalassiosira pseudonana*. *The ISME J.* 5, 1057–
663 1060.
- 664 Mayor, D.J., Sharples, C.J., Webster, L., et al. 2013. Tissue and size-related changes in the fatty acid and
665 stable isotope signatures of the deep sea grenadier fish *Coryphaenoides armatus* from the Charlie-
666 Gibbs Fracture Zone region of the Mid-Atlantic Ridge. *Deep Sea Res. II* 98, 421-430.
- 667 Martin, P., Lampitt, R.S., Perry, M.J., Sanders, R., Lee, C., D’Asaro, E., 2011b. Export and mesopelagic
668 particle flux during a North Atlantic spring diatom bloom. *Deep-Sea Res. I* 58, 338–349.
- 669 Moore, C. M.; Mills, M. M.; Arrigo, K. R.; et al. 2013. Processes and patterns of oceanic nutrient
670 limitation. *Nat. Geosci.* 6, 701-710.
- 671 O’Brien, C. J., Peloquin, J.A., Vogt, M., Heinle, M., Gruber, N., et al., 2013. Global marine plankton
672 functional type biomass distributions: coccolithophores. *Earth Syst. Sci. Data*, 5, 259–276.
- 673 Parrish, C.C. 1987. Separation of aquatic lipid classes by Chromarod thin-layer chromatography with
674 measurement by Iatroscan flame ionization detection. *Can. J. Fish. Aquat. Sci.* 44, 722–731.
- 675 Paytan, A., McLaughlin, K., 2007. The Oceanic Phosphorus Cycle. *Chem. Rev.* 107, 563–576.
- 676 Paytan, A.; Cade-Menun, B. J.; McLaughlin, K.; Faul, K. L. Selective phosphorus regeneration of sinking
677 marine particles: evidence from ³¹P-NMR. *Mar. Chem.* 2003, 82, 55–70.
- 678 Pond, D.W., Tarling, G.A., Mayor, D.J. 2014. Hydrostatic pressure and temperature effects on the
679 membranes of a seasonally migrating marine copepod. *Plos One* 9, e111043.

Gašparović, B., Penezić, A., Lampitt, R.S., Sudasinghe, N., Schaub, T. 2018. Phospholipids as a component of the oceanic phosphorus cycle. *Mar. Chem.* 250, 70-80.

Pre-print version

- 680 Pependorf, K.J., Tanaka, T., Pujo-Pay, M., Lagaria, A., Courties, C., Conan, P. Oriol, L., Sofen, L.E.,
681 Moutin, T., Van Mooy, B.A.S., 2011. Gradients in intact polar diacylglycerolipids across the
682 Mediterranean Sea are related to phosphate availability. *Biogeosciences*, 8, 3733–3745.
- 683 Rhead, M.M., Eglinton, G., Draffan, G.H., England, P.J., 1971. Conversion of oleic acid to saturated fatty
684 acids in Severn Estuary sediments. *Nature* 232, 327–330.
- 685 Rontani, J.-F., 2008. Photooxidative and autoxidative degradation of lipid components during the
686 senescence of phototrophic organisms. In: Matsumoto, T. (Ed.), *Phytochemistry Research*
687 *Progress*. Nova Science Publishers, pp. 115–144.
- 688 Rontani, J.-F., Koblížek, M., 2008. Regiospecific Enzymatic Oxygenation of cis-Vaccenic Acid in the
689 Marine Phototrophic Bacterium *Erythrobacter* sp strain MG3. *Lipids* 43, 1065–1074.
- 690 Rontani, J.-F., Zabeti, N., Wakeham, S.G., 2009. The fate of marine lipids: Biotic vs. abiotic degradation
691 of particulate sterols and alkenones in the Northwestern Mediterranean Sea. *Mar. Chem.* 113, 9-
692 18.
- 693 Rontani, J-F, Charriere, B., Forest, A., Heussner, S., Vaultier, F., et al. 2012. Intense photooxidative
694 degradation of planktonic and bacterial lipids in sinking particles collected with sediment traps
695 across the Canadian Beaufort Shelf (Arctic Ocean). *Biogeosciences*, 9, 4787-4802.
- 696 Sebastián, M., Smith, A.F., González, J.M., Fredricks, H.F., Van Mooy, B., et al., 2016. Lipid remodelling
697 is a widespread strategy in marine heterotrophic bacteria upon phosphorus deficiency, *ISME J.* 10,
698 968–978.
- 699 Suzumura, M., 2005. Phospholipids in marine environments: a review. *Talanta* 66, 422–434.
- 700 Suzumura, M., Ingall, E.D. 2004. Distribution and dynamics of various forms of phosphorus in
701 seawater: insights from field observations in the Pacific Ocean
702 and a laboratory experiment. *Deep-Sea Res. I* 51, 1113–1130.
- 703 Slocombe, S.P., Ross, M., Thomas, N., McNeill, S., Stanley, M.S., 2013. A rapid and general method for
704 measurement of protein in micro-algal biomass. *Bioresource Technol.* 129, 51–57.

Gašparović, B., Penezić, A., Lampitt, R.S., Sudasinghe, N., Schaub, T. 2018. Phospholipids as a component of the oceanic phosphorus cycle. *Mar. Chem.* 250, 70-80.

Pre-print version

- 705 Tamelander, T., Aubert, A.B. Wexels Riser, C., 2012. Export stoichiometry and contribution of copepod
706 faecal pellets to vertical flux of particulate organic carbon, nitrogen and phosphorus. *Mar. Ecol.*
707 *Prog. Ser.* 459, 17–28.
- 708 Testerink, C., Munnik, T., 2011. Molecular, cellular, and physiological responses to phosphatidic acid
709 formation in plants. *J. Exp. Bot.* 62, 2349–2361.
- 710 Tyrrell, T., 1999. The relative influences of nitrogen and phosphorus on oceanic primary production.
711 *Nature*, 400, 525–531.
- 712 Van Mooy, B.A.S., Rocap, G., Fredricks, H.F., Evans, C.T., Devol, A.H., 2006. Sulfolipids dramatically
713 decrease phosphorus demand by picocyanobacteria in oligotrophic marine environments, *Proc.*
714 *Natl. Acad. Sci.*, 103, 8607–8612.
- 715 Van Mooy, B.A.S., Fredricks, H.F., Pedler, B.E., Dyhrman, S.T., Karl, D.M., et al., 2009. Phytoplankton
716 in the ocean use non-phosphorus lipids in response to phosphorus scarcity. *Nature* 458, 69-72.
- 717 Van Mooy, B.A.S., Fredricks, H.F., 2010. Bacterial and eukaryotic intact polar lipids in the eastern
718 subtropical South Pacific: Water–column distribution, planktonic sources, and fatty acid
719 composition. *Geochim. Cosmochim. Acta* 74, 6499–6516.
- 720 Wakeham, S.G., 1989. Reduction of stenols to stanols in particulate matter at oxic–anoxic boundaries in
721 sea water. *Nature* 342, 787–790.
- 722 Wakeham, S.G., 1995. Lipid biomarkers for heterotrophic alteration of suspended particulate organic
723 matter in oxygenated and anoxic water columns of the ocean. *Deep Sea Res. I* 10, 1749–1771.
- 724 Wakeham, S.G., Hedges, J.I., Lee, C., Peterson, M. L., Hernes, P.J., 1997. Compositions and transport of
725 lipid biomarkers through the water column and surficial sediments of the equatorial Pacific Ocean,
726 *Deep-Sea Res. II*, 44, 2131–2162.
- 727 Wallmann, K., 2010. Phosphorus imbalance in the global ocean? *Global Biogeochem. Cycles* 24, B4030.
- 728 Weaver, P.P.E., Wynn, R.B., Kenyon, N.H., Evans, J.M., 2000. Continental margin sedimentation, with
729 special reference to the north-east Atlantic margin. *Sedimentology* 47, 239–256.
- 730 Welschmeyer, N.A., 1994. Fluorometric analysis of chlorophyll a in the presence of chlorophyll b and
731 pheopigments. *Limnol. Oceanogr.* 39, 1985–1992.

Gašparović, B., Penezić, A., Lampitt, R.S., Sudasinghe, N., Schaub, T. 2018. Phospholipids as a component of the oceanic phosphorus cycle. *Mar. Chem.* 250, 70-80.

Pre-print version

- 732 Williams, R.G., Roussenov, V., Follows, M.J., 2006. Nutrient streams and their induction into the mixed
733 layer. *Global Biogeochem. Cycles* 20, GB1016.
- 734 Wu, J.F., Sunda, W. Boyle, E.A., Karl D.M., 2000. Phosphate depletion in the western North Atlantic
735 Ocean. *Science* 289, 759–762.
- 736 Yamaguchi A., Watanabe, Y., Ishida, H., Harimoto, T., Furusawa, K., Suzuki, S., Ishizaka, J., Ikeda, T.,
737 Mac Takahashi M., 2002. Structure and size distribution of plankton communities down to the
738 greater depths in the western North Pacific Ocean. *Deep–Sea Res. II* 49, 5513–5529.
- 739 Yamaguchi, A., Watanabe, Y., Ishida, H., Harimoto, T., Maeda, M., Ishizaka, J., Ikeda, T., Takahashi,
740 M.M., 2005. Biomass and chemical composition of net–plankton down to greater depths (0–5800
741 m) in the western North Pacific Ocean. *Deep–Sea Res. I* 52, 341–353.
- 742 Yoshimura, T., Nishioka, J., Saito, H., Takeda, S., Tsuda, A., Wells, M.L., 2007. Distributions of
743 particulate and dissolved organic and inorganic phosphorus in North Pacific surface waters. *Mar.*
744 *Chem.* 103, 112–121.